Journal of Computational Physics 230 (2011) 3270–3275

Contents lists available at ScienceDirect

Journal of Computational Physics

journal homepage: www.elsevier.com/locate/jcp

Short note

Straightforward high-order numerical dissipation via the viscous term for direct and large eddy simulation

Eric Lamballais [a,*], Véronique Fortuné [a], Sylvain Laizet [b]

[a] Institute PPRIME, Department of Fluid Flow, Heat Transfer and Combustion, Université de Poitiers, ENSMA, CNRS, Téléport 2 - Bd., Marie et Pierre Curie B.P. 30179, 86962 Futuroscope Chasseneuil Cedex, France
[b] Department of Aeronautics, Imperial College London, South Kensington Campus, London SW7 2AZ, UK

ARTICLE INFO

Article history:
Received 12 November 2010
Received in revised form 25 January 2011
Accepted 25 January 2011

Keywords:
Direct and large eddy simulation
High-order compact finite difference scheme
Numerical dissipation
Computational aeroacoustics
Hyperviscosity
Spectral vanishing viscosity

ABSTRACT

In this short note, we show how to use a highly accurate finite-difference scheme to compute second derivatives in the Navier–Stokes equations while ensuring targeted numerical dissipation. This approach, essentially non conservative, is shown to be close to an upwind method and is straightforward to implement with a negligible computational extra cost. The benefit offered by the resulting discrete operator is illustrated for the direct computation of sound in aeroacoustics and in the more general context of large-eddy simulation through connections with hyperviscosity and spectral vanishing viscosity.

1. Introduction

Direct and large eddy simulation (DNS/LES) of turbulent flow is well known to require highly accurate numerical methods to preserve the fidelity of the physics without being overly demanding in computational resources. For geometry allowing the use of highly structured computational mesh, DNS/LES codes are frequently based on high-order schemes without dissipation error through the use of a centered formulation. However, the loss of accuracy introduced by numerical schemes at small scales combined with aliasing errors and other numerical artefacts (boundary conditions, failure of conservation properties at the discrete level, etc.) frequently lead to spurious oscillations at small scales, typically those close to the mesh size. These oscillations, often called "wiggles", can be controlled by the physical dissipation using a highly refined mesh, leading to a drastic increase of the computational cost.

To avoid this major drawback, various techniques are commonly used to suppress or reduce wiggles at marginal resolutions. The robustness of the computational procedure can be improved by a relevant choice for the formulation of the governing equations in order to ensure some conservation properties [30,15] or through the mesh arrangement (staggered mesh, see for instance [2,27]). The most popular method to control spurious oscillations is to use upwind schemes to compute the convective terms in order to reinforce artificially the dissipation near the mesh cutoff wavenumber. A similar effect can be obtained using a specific artificial damping term [16,33] or a filtering procedure [9,5,4]. Upwinding, damping or filtering techniques are essentially non-conservative methods that introduce more or less explicitly some numerical

* Corresponding author.
E-mail addresses: lamballais@univ-poitiers.fr, eric.lamballais@univ-poitiers.fr (E. Lamballais), veronique.fortune@univ-poitiers.fr (V. Fortuné), s.laizet@imperial.ac.uk (S. Laizet).

0021-9991/$ - see front matter © 2011 Elsevier Inc. All rights reserved.
doi:10.1016/j.jcp.2011.01.040

dissipation. For DNS, this artificial dissipation is dedicated to the control of wiggles. In implicit LES, it can also be interpreted as a subgrid modelling ensured by upwinding/damping [11] or filtering, this second technique being viewed as a relaxation model that can be used alone [24,31,5,4] or in conjunction with a deconvolution model [14,13]. Finally, let us mention that in the context of spectral methods, hyperviscosity can be used [6,12,21] to artificially extend the inertial range in a turbulent flow while ensuring some numerical dissipation near the mesh cutoff despite the artefacts discussed by [17,10]. In the same spirit, the spectral vanishing viscosity method [32,18,28] can also be viewed as an alternative LES model which can control the smallest scales without extra-dissipation at large scales.

The purpose of this paper is to propose a very simple scheme that can introduce straightforwardly some numerical dissipation without the use of any upwinding, damping or filtering operator. In practice, the extra-dissipation is directly enclosed in the viscous term of the Navier–Stokes equations through a specific finite difference scheme for the computation of second derivatives. The singular behaviour obtained at small scales for compact scheme is used here to freely adjust the level of numerical dissipation near the mesh cutoff while ensuring high-accuracy (virtually free from any numerical dissipation) at large scales. The excellent spectral property of the scheme will be shown through similarities with previous high-order upwind approaches. The ability of the resulting discretization error to behave like a spectral viscosity will also be exhibited.

2. Numerical dissipation via the second derivative approximation

For the second derivative, the 3–7 stencil[1] formulation

$$\alpha f''_{i-1} + f''_i + \alpha f''_{i+1} = a\frac{f_{i+1} - 2f_i + f_{i-1}}{\Delta x^2} + b\frac{f_{i+2} - 2f_i + f_{i-2}}{4\Delta x^2} + c\frac{f_{i+3} - 2f_i + f_{i-3}}{9\Delta x^2} \tag{1}$$

leads to a four parameters (α, a, b, c) finite difference scheme that can be at the best eighth-order accurate through the four constraints: (i) $a + b + c = 1 + 2\alpha$ (Δx^2 condition); (ii) $a + 4b + 9c = 12\alpha$ (Δx^4 condition); (iii) $a + 16b + 81c = 30\alpha$ (Δx^6 condition); (iv) $a + 64b + 729c = 56\alpha$ (Δx^8 condition). Here, $f_i = f(x_i)$, $f'_i = f'(x_i)$ and $f''_i = f''(x_i)$ denote the values of the function $f(x)$ and its first $f'(x)$ and second $f''(x)$ derivatives at the nodes $x_i = (i-1)\Delta x$ where Δx is the uniform mesh spacing.

In the framework of Fourier analysis, it is well known that a modified square wavenumber k'' can be related to the scheme (1) with the expression

$$k''\Delta x^2 = \frac{2a[1 - \cos(k\Delta x)] + \frac{b}{2}[1 - \cos(2k\Delta x)] + \frac{2c}{9}[1 - \cos(3k\Delta x)]}{1 + 2\alpha\cos(k\Delta x)} \tag{2}$$

The main purpose of this short note is to show how numerical dissipation can be directly controlled without the need of any upwinding procedure or additional discrete operator. The basic idea is to notice that k'' in (2) admits one singularity for $\alpha = 1/2$ at the cutoff wavenumber $k_c\Delta x = \pi$. The option proposed here is to freely adjust α and then control the shape of k'' while preserving the sixth-order accuracy through relationships (i, ii, iii). In practice, we can take advantage of the singularity of k'' to increase as much as required k'' near the cutoff wavenumber k_c through $\alpha \to 1/2$. Noting k''_c the expected value of k'' at the cutoff wavenumber, i. e. $k''|_\pi = k''_c$, it is easy to show that this condition combined with the sixth-order accuracy can be satisfied using the set of coefficients

$$\alpha = \frac{272 - 45k''_c\Delta x^2}{416 - 90k''_c\Delta x^2}, \quad a = \frac{48 - 135k''_c\Delta x^2}{1664 - 360k''_c\Delta x^2}, \quad b = \frac{528 - 81k''_c\Delta x^2}{208 - 45k''_c\Delta x^2}, \quad c = \frac{-432 + 63k''_c\Delta x^2}{1664 - 360k''_c\Delta x^2} \tag{3}$$

To illustrate the accuracy and flexibility of the resulting scheme, a set of $k''\Delta x^2$ is plotted in Fig. 1 for $k''_c\Delta x^2 = n\pi^2$, where n is an integer with $n = 1, \ldots, 10$. The conventional sixth-order compact scheme with $c = 0$ [23] (leading to $k''_c\Delta x^2 = 48/7$ with a sub-dissipative behaviour) is also presented for comparison. It can be observed that the range of high wavenumbers where k'' overestimates the exact value k^2 remains remarkably narrow even when the overestimation is strong (e.g. $n = 10$). In practical applications, the use of high value for n (leading to the quasi-singular condition $\alpha \approx 1/2$) would simply require an implicit time marching to avoid the numerical stability limit $\nu\Delta t/\Delta x^2 < \sigma_r/n\pi^2$ (with for instance $\sigma_r = 2.5$ for a RK3 scheme) in the framework discussed later in Section 3.

For some specific DNS/LES applications, it can be useful to extend this over-dissipation in a wider range. To illustrate this point without any stencil extension, the sixth-order constraint (iii) can be sacrificed leaving free two parameters among (α, a, b, c) to preserve a fourth-order accuracy. Then, two additional relationships can be chosen through for instance the condition on k'' at the cutoff wavenumber but also at an intermediate scale like $k\Delta x = 2\pi/3$, namely $k''|_{2\pi/3} = k''_m$. It is easy to show that the relationships (i, ii) combined with these two requirements lead to the set of coefficients

$$\begin{aligned} \alpha &= \frac{64k''_m\Delta x^2 - 27k''_c\Delta x^2 - 96}{64k''_m\Delta x^2 - 54k''_c\Delta x^2 + 48}, \quad a = \frac{54k''_c\Delta x^2 - 15k''_c\Delta x^2 k''_m\Delta x^2 + 12}{64k''_m\Delta x^2 - 54k''_c\Delta x^2 + 48} \\ b &= \frac{192k''_m\Delta x^2 - 216k''_c\Delta x^2 + 24k''_c\Delta x^2 k''_m\Delta x^2 - 48}{64k''_m\Delta x^2 - 54k''_c\Delta x^2 + 48}, \quad c = \frac{54k''_c\Delta x^2 - 9k''_c\Delta x^2 k''_m\Delta x^2 - 108}{64k''_m\Delta x^2 - 54k''_c\Delta x^2 + 48} \end{aligned} \tag{4}$$

The interest of the corresponding scheme will be shown in the next sections.

[1] Present approach can be easily generalized for other stencils.

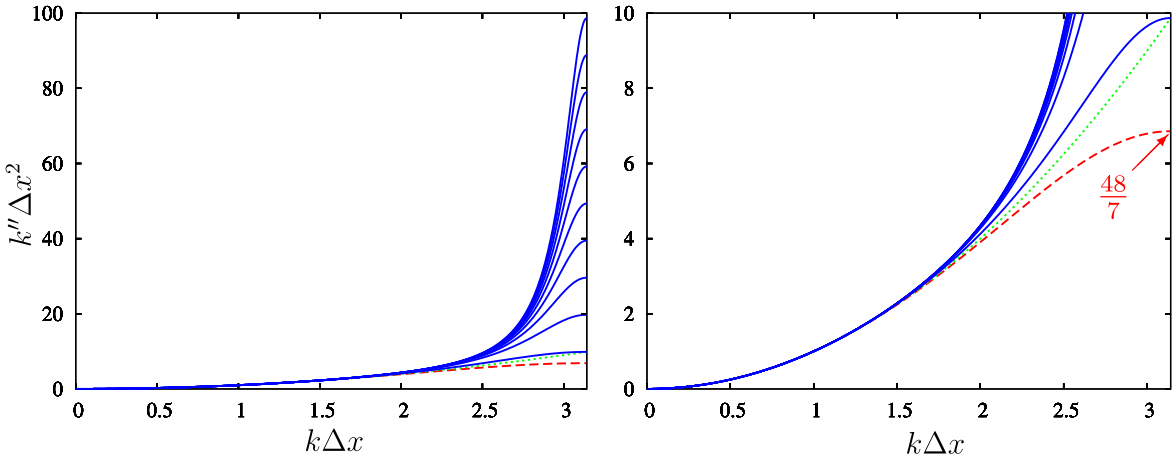

Fig. 1. Modified square wavenumbers $k''\Delta x^2$ for the sixth-order scheme (1), (3) imposing $k_c''\Delta x^2|_\pi = n\pi^2$ with $n = 1,\ldots,10$ (blue solid line, from bottom to top) compared with the exact square wavenumber $k^2\Delta x^2$ (green dotted line) and with the conventional sixth-order scheme $(1, c = 0)$ (red dashed line). The right plot is a zoom of the left one. (For interpretation of the references to colour in this figure legend, the reader is referred to the web version of this article.)

3. Comparison for a convection/diffusion equation

In the framework of Fourier analysis, it is well known that solving a linear convection/diffusion equation of the form $\frac{\partial u}{\partial t} = -c\frac{\partial u}{\partial x} + \nu\frac{\partial^2 u}{\partial x^2}$ using finite difference schemes provides a semi-discretized solution $u(x_i,t) = \exp\left[\imath k(x_i - c\frac{k_R'}{k}t)\right]$ $\exp[-(\nu k'' - ck_I')t]$ where $k' = k_R' + \imath k_I'$ and k'' are the modified wavenumbers related to the first and second derivative approximations respectively. Due to the centered formulation of (1), k'' is real (as its exact value of reference k^2) whereas k' can be complex, allowing the possibility to consider backward differences. The comparison between these approximations and the exact solution $u(x,t) = \exp[\imath k(x - ct)]\exp(-\nu k^2 t)$ leads to the natural distinction between dispersion and dissipation errors. Here, we focus on the dissipation error defined as $E_{diss} = \frac{k''-k^2}{k^2} - Re_{\Delta x}\frac{k_I'}{k^2\Delta x}$ where $Re_{\Delta x} = c\Delta x/\nu$ is the mesh Reynolds number.

The purpose of this section is to show that the scheme (1) used with the set of coefficients (3), (4) introduces a numerical dissipation similar to the one obtained using an upwind scheme. For instance, Fig. 2 presents the numerical dissipation obtained using the fifth-order upwind schemes of [29] or [1] combined with a conventional sixth-order compact scheme $(1, c = 0)$ for the second derivative with a typical mesh Reynolds number $Re_{\Delta x} = 200$. In the same figure, the numerical dissipation provided by the scheme (1), (3) or (1), (4) alone is also presented. The coefficients of these schemes have been adjusted to provide the same dissipation error $E_{diss}|_\pi$ at the cutoff wavenumber using (3) and with an additional constraint on $E_{diss}|_{2\pi/3}$ using (4). Compared with the two upwind combinations, the numerical dissipation introduced by the sixth-order scheme given by (1), (3) is found to be more concentrated near the cutoff, allowing the same efficiency for the control of

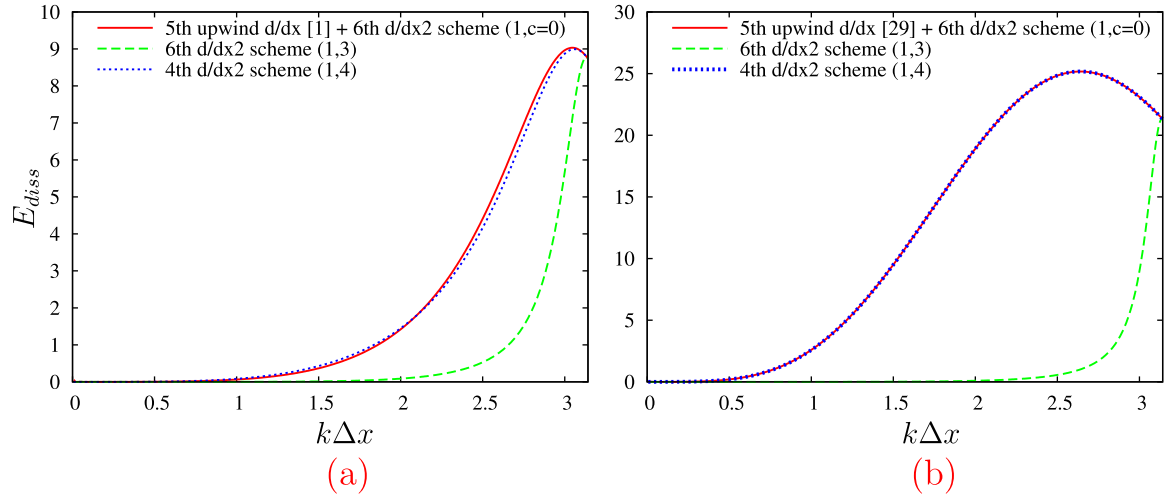

Fig. 2. Dissipation error E_{diss} for upwind schemes [1,29] combined with a conventional sixth-order compact scheme $(1, c = 0)$ to compute the second derivative and for the present schemes (1), (3) or (1), (4) at $Re_{\Delta x} = 200$.

grid-to-grid oscillations while being significantly less intrusive over a wide range of wavenumbers. It is worth noting that this favourable behaviour can be obtained without any optimization procedure. In contrary, for applications where a more extended numerical dissipation is expected, the fourth-order given by (1), (4) is found to mimic remarkably well the two fifth-order upwind schemes considered here, as far as a linear convection/diffusion equation is concerned.

4. Analogy with hyperviscosity and spectral vanishing viscosity

Due to the flexibility of the present viscous operator, it has also the potential to be used to mimic the subgrid-scale dissipation in the context of LES. In particular, the numerical dissipation can be viewed as a spectral viscosity. In practice, to be meaningful, the dissipation introduced by the discrete operator $\nu k''$ has to be compared with the exact one (free from discretization error) $(\nu + \nu_s)k^2$ where ν and ν_s are the molecular and spectral viscosity respectively. Then, a spectral viscosity ν_s'' associated with the discretization error can be introduced by the expression $(\nu + \nu_s'')k^2 = \nu k''$ leading to the definition $\nu_s'' = \nu(k'' - k^2)/k^2$. This expression can be compared with a hyperviscosity expressed as $\nu_s = \nu_0\, k^{2n-2}$ where n and ν_0 are the power and coefficient of the hyperviscous operator respectively. An example of the agreement obtained is presented in Fig. 3 (a) for the case $n = 4$ and $\nu/\nu_0 = 0.01$ using the fourth-order scheme (1), (4) with a coefficient calibration to fit the hyperviscosity at $k = k_c$ and $k = 2k_c/3$. In particular, it can be observed that the present scheme is more representative of a hyperviscosity over the full range $k \in [0, k_c]$ compared with an iterated sixth-order scheme $(1, c = 0)$ which is, in addition, significantly more expensive in terms of computational time. As a consequence, in the context of isotropic turbulence, the energy hyperdissipation $\varepsilon = 2\nu_0 \int_0^{k_c} k^{2n} E(k)dk$ is clearly more accurately estimated using the scheme (1), (4) than using an iterated discrete Laplacian operator discretized with a conventional scheme (see Fig. 3, a).

In the same spirit, the fourth-order scheme (1), (4) can be used to mimic a spectral vanishing viscosity (SVV) operator. Two examples of comparison between the discrete spectral viscosity ν_s'' associated with the scheme (1), (4) and the SVV expressed as $\nu_s(k) = \nu_0 \exp\left[-\left(\frac{k_c - k}{0.3k_c - k}\right)^2\right]$ are presented in Fig. 3 (b). Both schemes are adjusted to lead to the same dissipation at the cutoff wavenumber while being more or less concentrated in the small scale range. The ability of the scheme (1), (4) to mimic a SVV operator is acceptable even if the separation between the dissipative range and the viscosity-free large scales is less sharp. To better fit SVV at small wave numbers using the scheme (1), (4), it is necessary to shorten the dissipative range, so that the global dissipation is also reduced as shown in Fig. 3 (b). In conclusion, the present scheme can be viewed as a very simple extension of the SVV approach to finite-difference methods. A secondary advantage of this extension is that both molecular and spectral viscosity effects are included in a single operator with again no significant computational extra-cost compared with a conventional viscous operator. Naturally, other kernels of spectral viscosity can be considered, as for instance the "cusp behaviour" [22] in a spectral eddy viscosity model that can be easily reproduced (not shown) using the scheme (1), (4).

5. Applications

The dissipation properties of the sixth-order scheme (1), (3) have already been successfully used to carry out three-dimensional DNS of incompressible turbulent flows in a plane channel [19] and over a half-body through a laminar separation [20]. In this section, a more selective test case is considered in the context of direct computation of sound. This

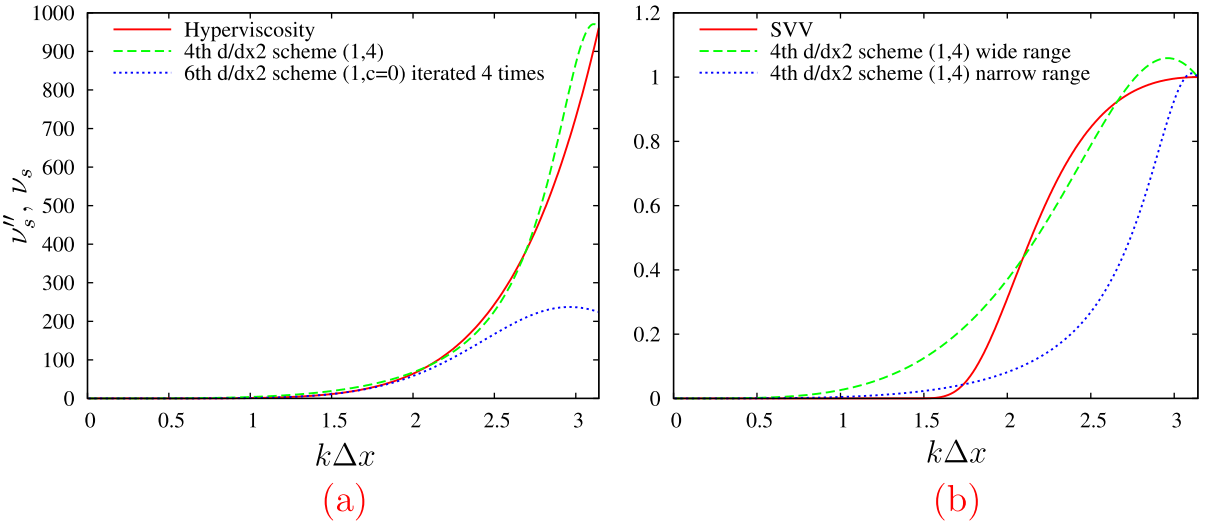

Fig. 3. Comparison among the spectral viscosity ν_s'' introduced by the scheme (1), (4), the hyperviscosity (a) and the SVV kernel (b).

framework is well known to be very demanding in terms of numerical accuracy, especially when spurious oscillations must remain weak with respect to low amplitude acoustic waves at moderate Mach numbers. Here, the sound emission of a canonical two-dimensional compressible mixing layer is considered by DNS using a code already validated for this specific flow configuration [25,7].

The mixing layer is spatially evolving between two free-streams of velocity $U_1 = 0.5c_2$ and $U_2 = 0.25c_2$ where c_2 is the sound speed of reference. The Reynolds number based on the velocity difference $U_1 - U_2$ and on the inflow vorticity thickness δ_ω is 400. The computational domain $L_x \times L_y = 800\delta_\omega \times 800\delta_\omega$ is discretized using $n_x \times n_y = 1035 \times 431$ mesh nodes on a Cartesian mesh stretched in x and y. This spatial resolution is marginal with a mesh Reynolds number $Re_{\Delta x} \approx 200$ in the shear region. Sixth-order compact centered schemes are used for the spatial differentiation. To obtain accurate non-reflecting boundary conditions, buffer zones with aerodynamic and acoustic dissipation/absorption are used [25].

Concerning the vortex dynamics reproduced by present DNS, vortex roll-up and pairings are observed as the flow develops further downstream. As already shown in the previous DNS studies of [8,3], these events, especially the pairing, generate acoustic waves that propagate in both sides of the mixing layer. These waves can be highlighted through a visualization of the fluctuating pressure, as shown in Fig. 4 (b) in good agreement with the reference results [8,3]. However, at the present marginal resolution, the lack of any numerical dissipation is found to prevent the production of reliable acoustic results, as illustrated in Fig. 4 (a) where spurious acoustic waves are found to contaminate the whole acoustic field. The exact production mechanism of these spurious acoustic waves is difficult to understand. A serious analysis would require to consider the interactions among the boundary condition treatment, the numerical errors and the sound generation due to the vortex dynamics. [7] have already shown the favourable behaviour of the upwind schemes of [1] that can suppress this acoustic contamination at marginal resolution. Here, it is shown that in a similar numerical configuration, the use of the sixth-order scheme (1), (3) can also control the spurious acoustic waves without the need of any upwinding (see Fig. 4, b). Naturally, for the description of highly nonlinear compressible phenomena like shocks, additional tests are required to confirm the ability of the present viscous operator to stabilize and regularize the corresponding oscillations.

As a second practical example, the ability of the scheme (1), (4) to be used as a SVV operator is considered. For this purpose, a LES of a turbulent channel flow is performed with a Reynolds number $Re_m = U_m h/\nu = 6882$ where U_m is the bulk velocity and h the half-width channel. The same flow configuration as the DNS of [26] is considered (computational domain of $L_x \times L_y \times L_z = 2\pi h \times 2h \times \pi h$ with periodicity in the longitudinal and spanwise directions x, z and no-slip conditions at $y = \pm h$) but using a coarse mesh $n_x \times n_y \times n_z = 64 \times 129 \times 48$. The grid is stretched in the normal y-direction with $0.9 < \Delta y^+ < 41$. The LES has been performed using the code "Incompact3d" [19] that solves the incompressible Navier–Stokes equations on a Cartesian mesh using high-order compact finite difference schemes [23]. The viscous term is discretized using the fourth-order scheme (1), (4) adjusted to mimic a SVV operator as shown in Fig. 3 (b) with $\nu/\nu_0 = 1/3$ or equivalently $k_c''\Delta x^2 = 4\pi^2$. The friction velocity obtained in this calculation lead to a nominal value of $h^+ = 390$, in excellent agreement with the reference value of $h^+ = 392$ reported in [26]. The benefit offered by the use of present SVV operator-like can be confirmed by the examination of the mean velocity profile (see Fig. 5, a) that is found to fit remarkably well the DNS data. A similar agreement of turbulent statistical data can be observed for the turbulent intensities presented in Fig. 5 (b). In

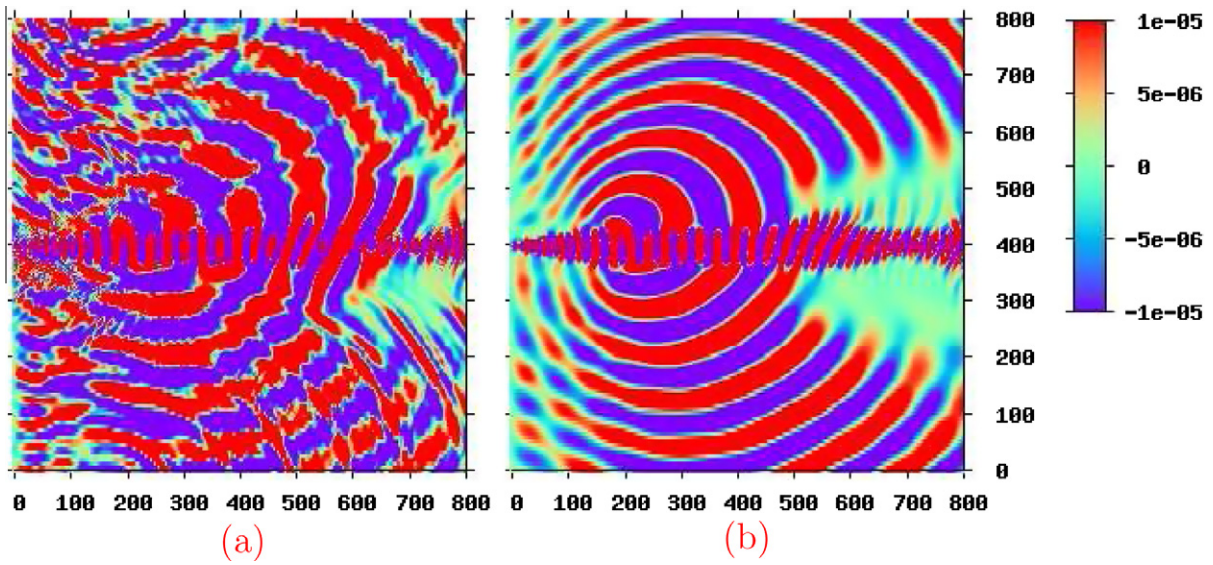

Fig. 4. Pressure map using conventional sixth-order centered schemes without numerical dissipation (a) or using the scheme (1), (3) for the calculation of second derivatives (b).

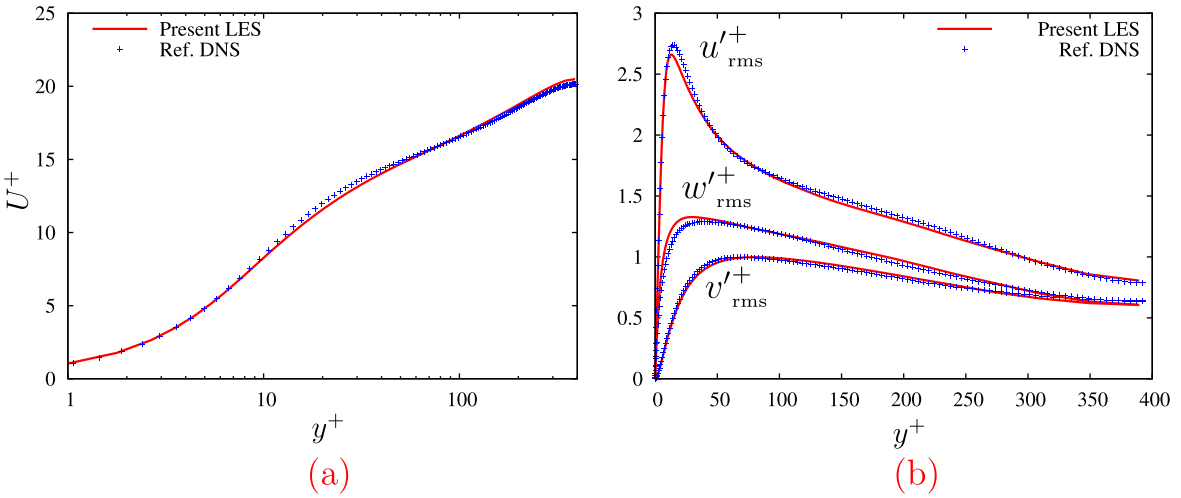

Fig. 5. Mean velocity and turbulent intensity profiles in a turbulent channel flow. Solid lines: LES using the scheme (1), (4) to provide a SVV operator-like. Symbols: reference DNS [26].

conclusion, these results indicate that the present high-order numerical dissipation can be helpful to perform accurate LES without any explicit modelling of subgrid scales, in the same spirit as an approach based on SVV.

Acknowledgements

This work was granted access to the HPC resources of IDRIS-CINES-CCRT under the allocation 2010-0210912 made by GENCI (Grand Equipement National de Calcul Intensif).

References

[1] N.A. Adams, K. Shariff, J. Comput. Phys. 127 (1996) 27–51.
[2] B.J. Boersma, J. Comput. Phys. 208 (2005) 675–690.
[3] C. Bogey, C. Bailly, AIAA J. 38 (12) (2000) 2210–2218.
[4] C. Bogey, C. Bailly, Comput. Fluids 35 (2006) 1344–1358.
[5] C. Bogey, C. Bailly, Phys. Fluids 18 (6) (2006) 1–14.
[6] V. Borue, S.A. Orszag, J. Fluid Mech. 366 (1998) 1–31.
[7] M. Cabana, V. Fortuné, E. Lamballais, in: V. Armenio, B.J. Geurts, J. Frölich, (eds.), Proceedings Direct and Large-Eddy Simulation VI, Springer, 2010, pp. 1–6, (ERCOFTAC series).
[8] T. Colonius, S.K. Lele, P. Moin, J. Fluid Mech. 330 (1997) 375–409.
[9] J. Freund, J. Fluid Mech. 438 (2001) 277–305.
[10] U. Frisch, S. Kurien, R. Pandit, W. Pauls, S.S. Ray, A. Wirth, J.-Z. Zhu, Phys. Rev. Lett. 101 (14) (2008) 1–4.
[11] C. Fureby, F.F. Grinstein, J. Comput. Phys. 181 (1) (2002) 68–97.
[12] N.E. Haugen, A. Brandenburg, Phys. Rev. E 70 (2) (2004) 1–7.
[13] S. Hickel, N.A. Adams, Phys. Fluids 19 (10) (2007) 1–13.
[14] S. Hickel, N.A. Adams, J.A. Domaradzki, J. Comput. Phys. 213 (1) (2006) 413–436.
[15] A.E. Honein, P. Moin, J. Comput. Phys. 201 (2004) 531–545.
[16] A. Jameson, W. Schmidt, E. Turkel, AIAA paper 1981-1259, 1981.
[17] J. Jimenez, J. Fluid Mech. 279 (1994) 169–176.
[18] G.-S. Karamanos, G.E. Karniadakis, J. Comput. Phys. 163 (11) (2000) 22–50.
[19] S. Laizet, E. Lamballais, J. Comput. Phys. 228 (2009) 5989–6015.
[20] E. Lamballais, J. Silvestrini, S. Laizet, Int. J. Heat Fluid Flow 31 (3) (2010) 295–306.
[21] A.G. Lamorgese, D.A. Caughey, S.B. Pope, Phys. Fluids 17 (1) (2005) 1–10.
[22] M. Lesieur, O. Métais, P. Comte, Large-Eddy Simulation of Turbulence, Cambridge University Press, 2005.
[23] S.K. Lele, J. Comput. Phys. 103 (1992) 16–42.
[24] J. Mathew, R. Lechner, H. Foysi, J. Sesterhenn, R. Friedrich, Phys. Fluids 15 (8) (2003) 2279–2289.
[25] C. Moser, E. Lamballais, Y. Gervais, AIAA paper, 2006-2447, 2006.
[26] R.D. Moser, J. Kim, N.N. Mansour, Phys. Fluids 11 (4) (1999) 943–945.
[27] S. Nagarajan, S.K. Lele, J.H. Ferziger, J. Comput. Phys. 191 (2003) 392–419.
[28] R. Pasquetti, J. Sci. Comput. 27 (1–3) (2006) 365–375.
[29] M.M. Rai, P. Moin, J. Comput. Phys. 96 (1991) 15–53.
[30] N. Sandham, Y. Yao, A. Lawal, J. Comput. Phys. 178 (2002) 307–322.
[31] P. Schlatter, S. Stolz, L. Kleiser, in: E. Lamballais, R. Friedrich, B.J. Geurts, O. Métais (Eds.), Direct and Large-Eddy Simulation VI, Springer, 2006, pp. 135–142. ERCOFTAC series.
[32] E. Tadmor, SIAM J. Numer. Anal. 26 (1) (1989) 1–30.
[33] C.K.W. Tam, J.C. Webb, Z. Dong, J. Comput. Acous. 1 (1) (1993) 1–30.